

A Novel Technique for Induction Motor Rotor Broken Bars Diagnosis in Special Variable Speed Drives

H.H. Hanafy¹, A. M. Hussien², E. A. El-Zahab³, M. O. Khalil⁴

^{1,3,4}*Electrical Power and Machines Department, Faculty of Engineering, Cairo University, Egypt*

²*Electrical Research Department, Mechanical and Electrical Research Institute, Egyptian Ministry of Public Works and Irrigation, Egypt*

¹*Hanafy_Hassan@hotmail.com* ²*hussien_25@yahoo.com* ³*zahab0@yahoo.com* ⁴*m.khalil20@yahoo.com*

(Received 12/3/2009; accepted for publication 5/6/2009)

Abstract. This paper deals with diagnosis of induction motor broken bar fault supplied from a special variable speed drive (VSD) equipped with an AC reactor and a sine-wave shaping filter on the output side, which could not be avoided due to vibration limits of the supporting construction. The proposed method is the instantaneous power spectrum analysis technique combined with the mean absolute difference (MAD) approach. The experimental results show that the instantaneous power spectrum analysis method is only effective when the motor is supplied from a sinusoidal supply, in contrast to the demonstrated VSD. The instantaneous power spectrums of the healthy rotor case and the broken bar rotor cases is processed with MAD algorithm to investigate the similarity between them. The results show that this combined technique is highly effective in diagnosis of broken rotor bar fault in case of the special VSD.

Keywords: Faulty induction motor, Broken bars diagnosis, Mean absolute difference

1. Introduction

The history of fault diagnosis and protection is as archaic as the machines themselves. The manufacturers and users of electrical machines initially relied on simple protection such as over-current, over-voltage, earth-fault, etc. to ensure safe and reliable operation. However, as the tasks performed by these machines grew increasingly complex, improvements were also sought in the field of fault diagnosis. It has now become very important to diagnose faults at their very inception; as unscheduled machine downtime can upset deadlines and cause heavy financial losses.

In [1-2] the authors reviewed a large number of publications dealing with the induction motor faults. Generally, various monitoring techniques for fault detection were used by researchers. The air-gap torque spectrum is a potential signature for online condition monitoring and fault diagnosis [3]. A comparison and performance evaluation of different diagnostic procedures that use input electric signals to detect and quantify rotor breakage in induction machines supplied by the mains has been presented in [4]. One of the most well-known approaches regarding the diagnosis of rotor faults in induction machines is based on online monitoring and processing of the stator currents to detect typical spectrum lines. The main advantages and drawbacks of motor current signal processing techniques for induction motor rotor fault detection (mainly broken bars and bearing deterioration) has been presented in [5]. A study describes broken bar detection in induction motors without using additional sensor but is based on observation of the fluctuations of stator current zero crossing times has been presented in [6]. In [7] a study dealing with mixed broken rotor bars and eccentricity faults in squirrel cage induction motors using instantaneous power spectrum has been presented. Diagnosis based on the global fault index method applied to the instantaneous power signal and line current signal provides relevant results for the detection of broken rotor bars has been presented in [8]. The application of a Time-Stepping Coupled Finite Element-State Space (TSCFE-SS) model for predictive non-invasive diagnosis and characterization of effects of rotor broken bars and end-ring connector segments has been presented in [9]. It was found that faults due to broken bars degrade the magnetic force distribution on the rotor bars and the core loss distribution on the rotor tooth adjacent to broken bars, and the bars adjacent to broken bars will become more susceptible to additional wear and eventual breaking [10]. Induction motor fault diagnosis method based on three-phase stator current envelopes for broken rotor bars and inter-turn short circuits has been presented in [11]. The performances of voltage unbalance and rotor fault detections using an external stray flux sensor in a working three-phase induction machine has been presented in [12].

In this paper an experimental study of the instantaneous power spectrum technique in case of sinusoidal supply and the same technique combined with the mean absolute difference approach in case of special VSD for the diagnosis of the broken bar fault are applied for the following cases; one broken bar and two adjacent broken bars. Results of each supply case will be compared with the healthy cage result for the same supply and load conditions. The results show that this combined technique is highly effective in diagnosis of broken rotor bar fault in case of VSD.

2. Instantaneous Power Signature Technique

Assuming an ideal three phase voltage supply with instantaneous phase voltage of $v_s(t)$ and healthy motor with no speed oscillation, and an instantaneous phase current of $i_s(t)$, the instantaneous power $P_s(t)$ can be written as follows [8]:

$$v_s(t) = \sqrt{2}V_s \cos(\omega t) \quad (1)$$

$$i_s(t) = \sqrt{2}I_s \cos(\omega t - \varphi) \quad (2)$$

$$p_s(t) = V_s I_s [\cos(2\omega t - \varphi) + \cos(\varphi)] \quad (3)$$

Where φ = the motor phase angle.

As shown from (2) and (3), the current spectrum has only one component at $f_s = \omega/2\pi$, while the power spectrum has two components, DC component and the other component at $f_c = \omega/\pi$. when a bar breaks, a rotor asymmetry occurs. Causing the appearance of additional two frequency components, the lower component is due to the backward rotating field resulting from the broken bar fault and the upper component is due to speed oscillation and torque pulsation. These components occur at frequencies given by [2], [8]:

$$f_{bb} = (1 \pm 2K s) f_s \quad (4)$$

Where:

$$K = 1, 2, 3, \dots$$

s = operating per unit slip of the motor.

The lower frequency component magnitude is not equal to the upper component [7-8]. So in case of broken bars, the mathematical expression of the instantaneous power of a squirrel cage induction motor is given by [8]:

$$\begin{aligned} p_s(t) &= p_1(t) + p_2(t) + p_3(t) \\ p_1(t) &= VsIs [Cos(2\omega t - \phi) + Cos\phi] \\ p_2(t) &= \sum_{K=1}^{\infty} VsI_{bpk} \{Cos((2-2ks)\omega t - \phi_{bpk}) + Cos(2ks\omega t + \phi_{bpk})\} \\ p_3(t) &= \sum_{K=1}^{\infty} VsI_{bnk} \{Cos((2+2ks)\omega t - \phi_{bnk}) + Cos(2ks\omega t - \phi_{bnk})\} \end{aligned} \quad (5)$$

Where

I_{bpk} : RMS value of the current component at frequency $(1-2ks)f_s$

I_{bnk} : RMS value of the current component at frequency $(1+2ks)f_s$

ϕ_{bpk} : Initial phase angle of the current component at the frequency $(1-2ks)f_s$

ϕ_{bnk} : Initial phase angle of the current component at the frequency $(1+2ks)f_s$

3. Mean Absolute Difference Approach

The Mean Absolute Difference (MAD) is widely used in signal processing applications to investigate the similarity between two vectors. In most cases, the MAD [13] approach did not show better performance than the sophisticated schemes such as finite element method or neural networks [9-10], [17]. However it is often used for real-time implementation, because it is computationally very efficient. In our proposed method, the MAD is used to investigate the un-similarity between two vectors, these vectors are the instantaneous power spectrum of the predetermined reference vector (healthy cage) and the examined vectors (broken bars cages) at different speeds (VSD). The MAD formula is given by [13]

$$MAD = \frac{1}{n} \sum_{m=0}^{n-1} |A_m - B_m| \quad (6)$$

Where:

n : Length of the vectors

A_m : Reference vector (Healthy case)

B_m : Examined vector for each case

4. Experimental Results and discussion

The motor under test has been chosen as 3 HP, 2-pole, 380 V and 50 Hz cage induction motor driving a water pump with load characteristics as shown in Fig.(1). The test bed block diagram is shown in Fig.(2), which consists of current and voltage transducers from LEM and their part numbers are LTS 25-NP and LV 100-400 respectively. The data acquisition system is NI PCI-6251 16-Bit, 1 MS/s with connection board connected to an IBM compatible PC. The diagnosis software is implemented on NI LabView v.8 [14-15]; the results documentation, formatting, using NI Diadem V.10 [16]. The stator voltages and currents were sampled at 20 KHz individually for 10 seconds of steady state operation, which gives a 0.1 Hz spectrum resolution with 10 KHz full scale spectrum. Voltage and current waveforms are multiplied together to get the instantaneous power waveform and fast Fourier transform is applied.

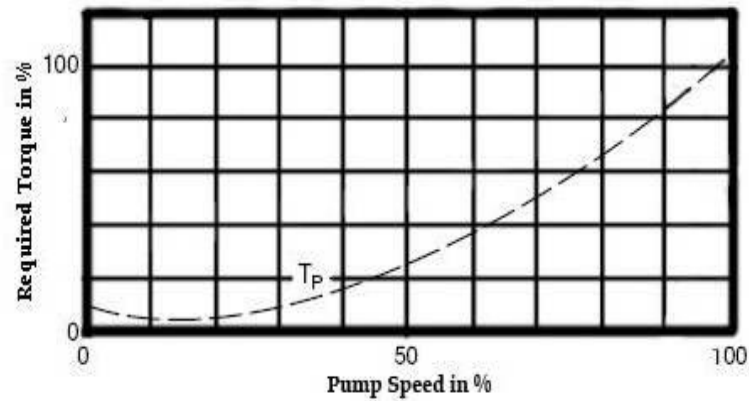


Fig.(1). Torque-Speed characteristics of the mechanical load (Pump).

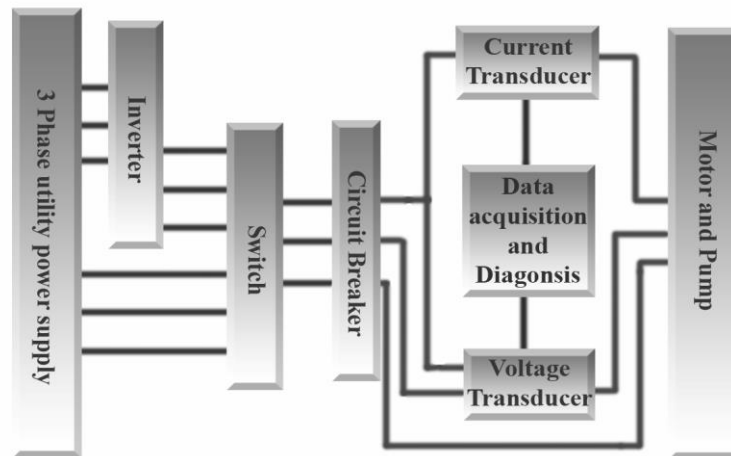


Fig.(2). Test bed block diagram.

The experimental data limited to frequency components $(2 \pm 2ks)f_s$, with $k=1,2$ and discussions are demonstrated in sections as follows:

- A) Instantaneous Power of healthy and broken cage bars in case of sinusoidal supply.
- B) Instantaneous Power of healthy and broken cage bars in case of VSD.
- C) The proposed combined technique.

A) Instantaneous Power of Healthy and Broken Cage Bars in Case of Sinusoidal Supply

Fig.(3) shows the instantaneous power spectrum of the healthy cage with existing lower and upper sideband frequency components, these components exist even in the healthy case due to magnetic and electrical asymmetries from the manufacturing process. Figs.(4-5) show the instantaneous power spectrum of the broken bar cage cases.

According to the results, a moving average scheme is applied which will be the reference instead of the zero point. Table (1) shows the amplitude of the sideband components referenced from the calculated average and the speed of each case.

From table (1) and figs. (3-5), the broken bar fault can be easily detected by noticing the amplitude of the sideband components (for different fault cases there is boosting in the sidebands amplitude), which shows that the instantaneous power method is highly effective in diagnosis of the broken bar fault under different fault cases when the voltage source is a normal three phase commercial supply.

Table (1). Amplitude of the sideband components referenced from the calculated average and the speed of each case.

Motor Status	K=1 left (dB)	K=1 right (dB)	K=2 left (dB)	K=2 right (dB)	Speed (rpm)
Healthy	0.62	3.24	14.07	13.93	2970
One Broken Bar	20.74	23.08	17.58	16.94	2943
Two Adj. Broken Bars	24.41	29.44	22.29	17.8	2930

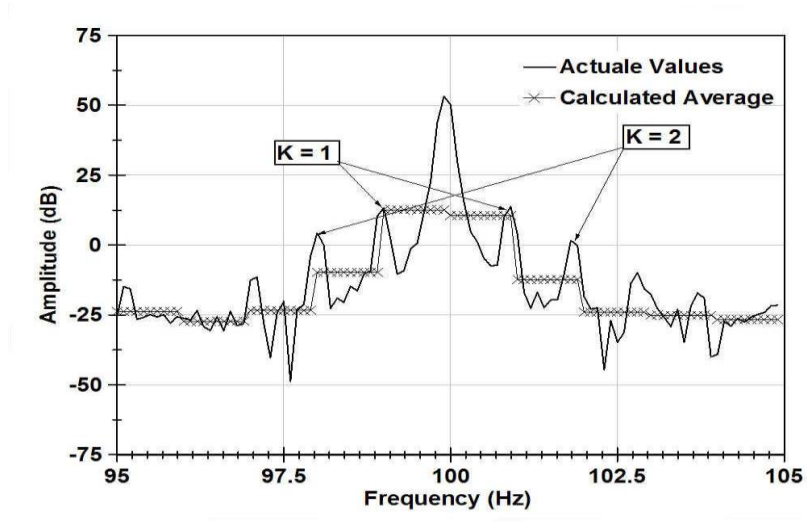


Fig.(3). Instantaneous power spectrum of healthy cage for sinusoidal supply.

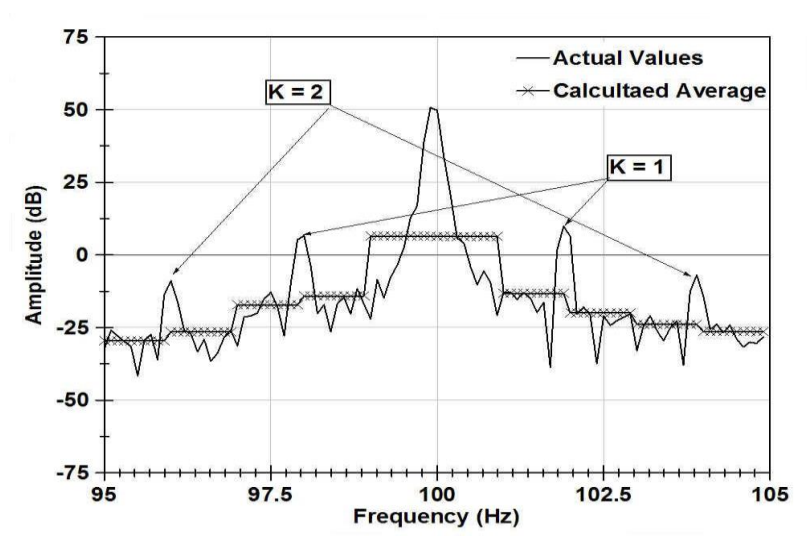


Fig.(4). Instantaneous power spectrum of one broken bar cage for sinusoidal supply.

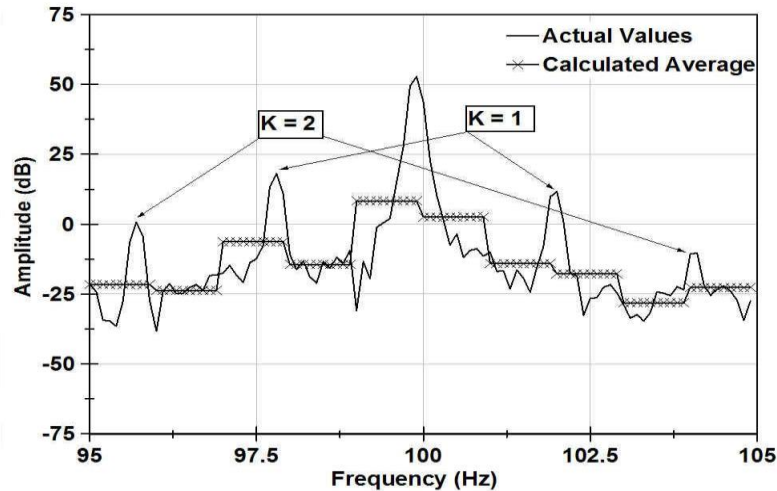


Fig.(5). Instantaneous power spectrum of two adjacent broken bars cage for sinusoidal supply.

B) Instantaneous Power of healthy and broken cage bars in case of VSD

The waveform of the inverter output voltage at 50 Hz is shown in fig.(6). Mainly the difference in the waveform from the traditional inverter is due to the built in output side AC reactor and Sin-wave shaping filter.

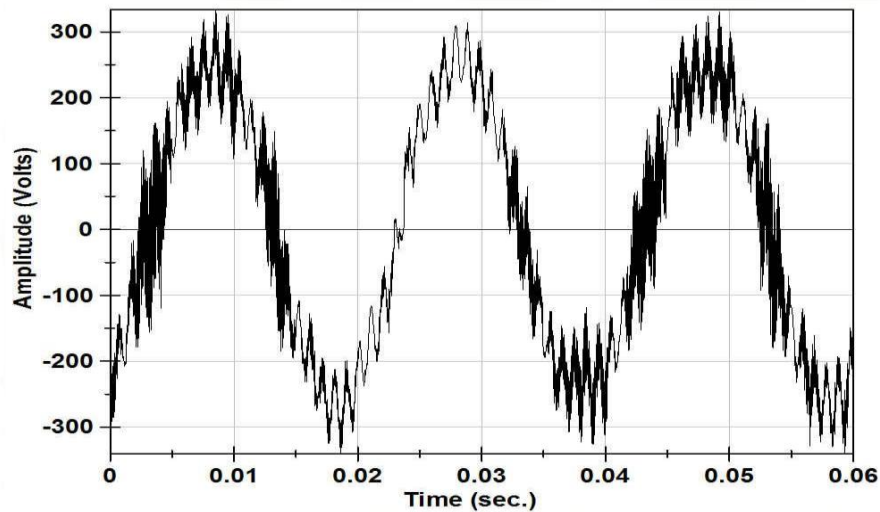


Fig.(6). Waveform of the inverter output voltage at 50 Hz.

The main function of the filter and the reactor is to reduce the vibration in the motor caused by inverter switching waveforms. This is the case of high power motor in range of 200 HP inverters, where the vibration consideration is important. The results shown in this section is the instantaneous power spectrums at the supply frequencies 45, 50 and 55 Hz. For the 45 Hz, figs.(7-9) show no identification sideband frequencies as in the case of the sinusoidal three phase supply. For the 50 Hz, figs.(10-12) show no identification sideband frequencies as the sinusoidal supply case. Also for the 55 Hz, figs (13-15) show no identification sideband frequencies.

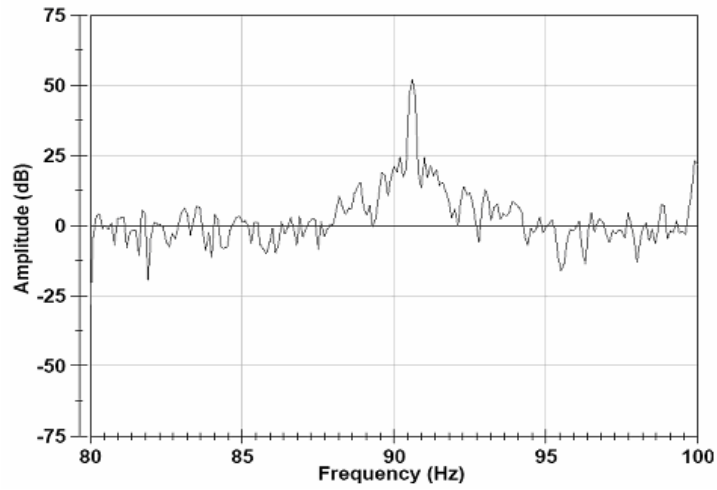


Fig.(7). Instantaneous power spectrum of healthy cage for inverter supply at 45 Hz.

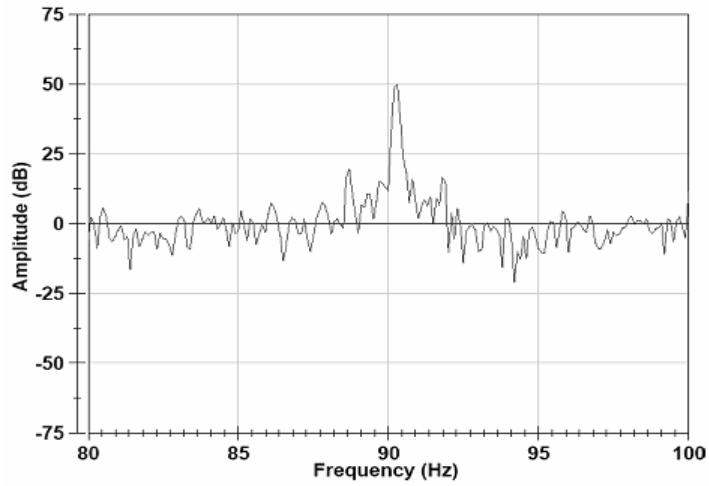


Fig.(8). Instantaneous power spectrum of one broken bar cage for inverter supply at 45 Hz.

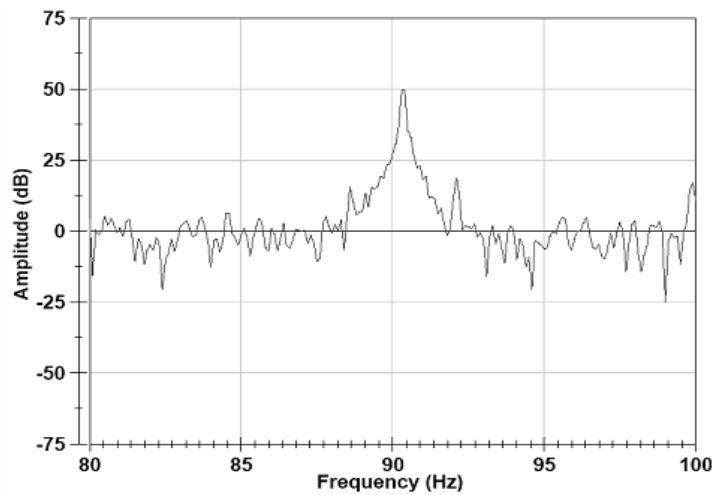


Fig.(9). Instantaneous power spectrum of two adjacent broken bars cage for inverter supply at 45 Hz

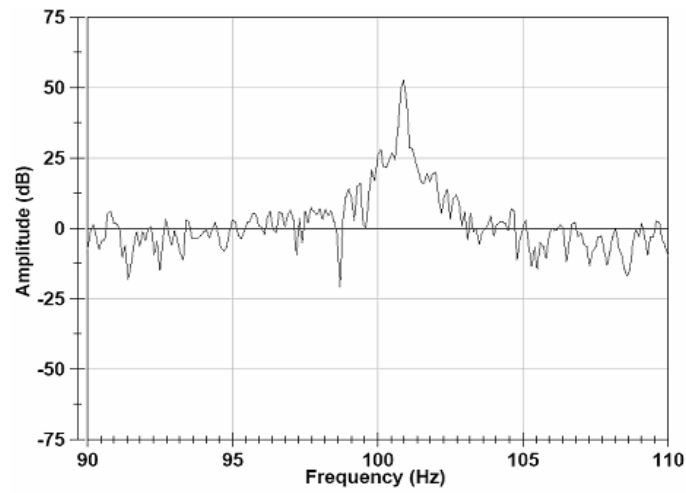


Fig.(10). Instantaneous power spectrum of healthy cage for inverter supply at 50 Hz.

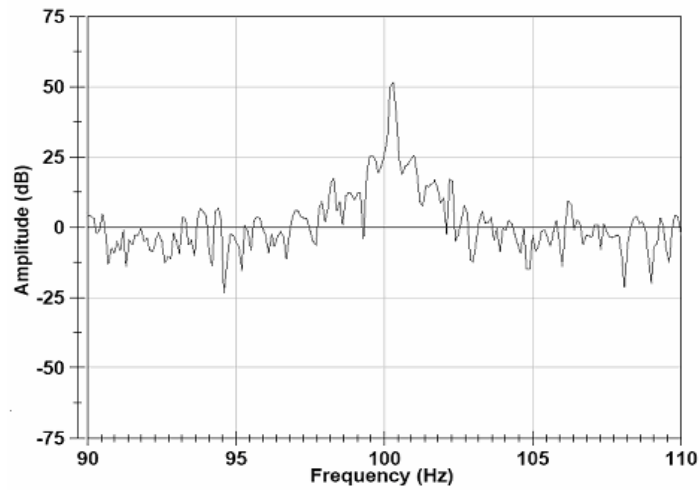


Fig.(11). Instantaneous power spectrum of one broken bar cage for inverter supply at 50 Hz.

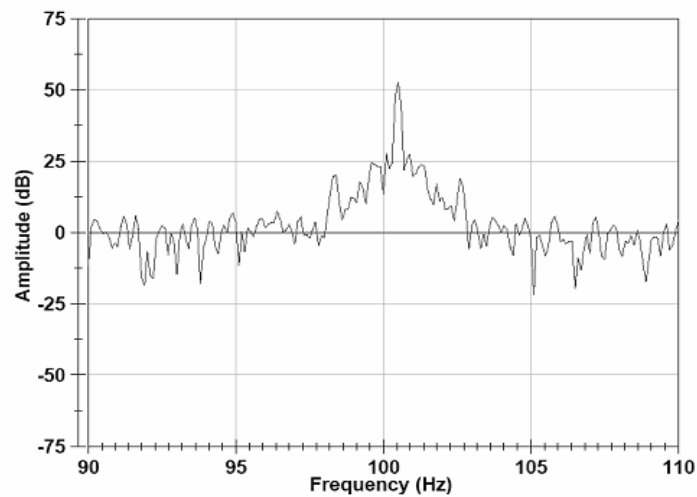


Fig.(12). Instantaneous power spectrum of two adjacent broken bars cage for inverter supply at 50 Hz.

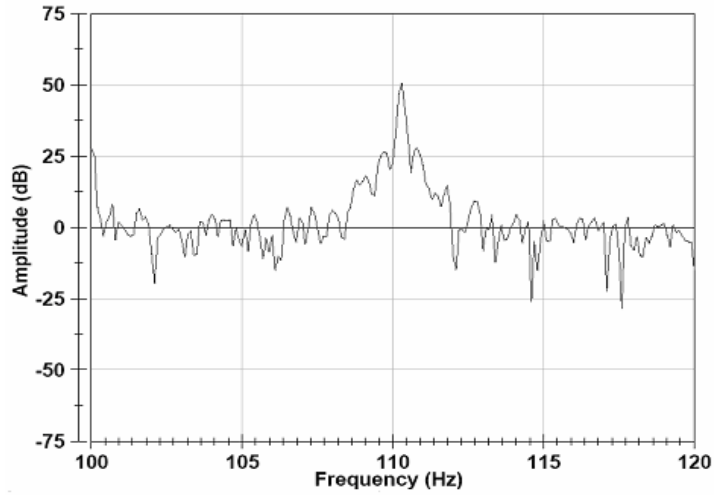


Fig.(13). Instantaneous power spectrum of healthy cage for inverter supply at 55 Hz.

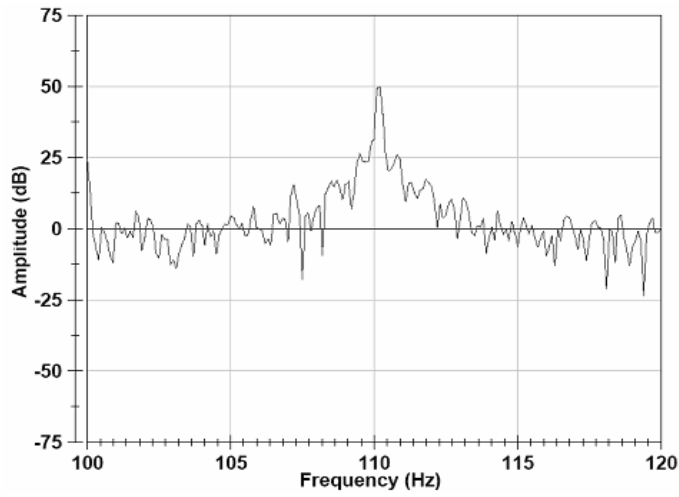


Fig.(14). Instantaneous power spectrum of one broken bar cage for inverter supply at 55 Hz.

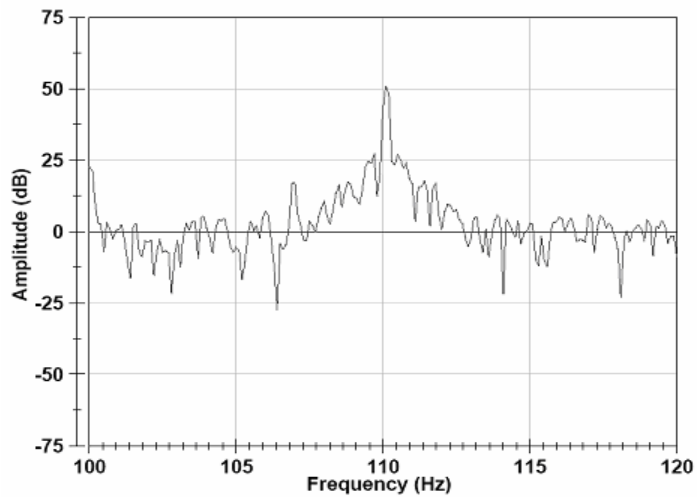


Fig.(15). Instantaneous power spectrum of two adjacent broken bars cage for inverter supply at 55 Hz.

According to these results, the instantaneous power spectrum method is not effective in the case of special inverter case, in contrast with the sinusoidal supply case.

C) The Proposed Combined Technique

In [13], the MAD was applied as follows; extract appropriate features that contain useful fault signature (upper and lower sideband) in the spectral information while suppressing other spectral information such as fundamental and noise components. After the appropriate features are extracted, the reference (healthy) and examined (broken bar) vectors are compared using (6) for detection of the broken bar fault.

In the proposed technique, The MAD was calculated as follows; the healthy, one broken bar and two adjacent broken bars cages instantaneous power was acquired using the proposed test-bed. The reference vector will be the instantaneous power spectrum of the healthy case, and the examined vector will be the instantaneous power spectrum of the faults cases, without removing any components from the spectrum. The MAD is used to search for hidden information in the spectrum. Table (2) shows MAD magnitudes versus supply frequency.

Fig.(16) shows the calculated MAD for one broken bar and two adjacent broken cage bars versus the supply frequency. It is clearly that the combined technique is highly effective in diagnosis of broken rotor bar fault in case of VSD.

Table (2). MAD magnitudes versus supply frequency.

Synchronous Frequency (Hz)	MAD of One Broken Bar (dB)	MAD of Two Adj. Broken Bars (dB)
35	6.71275	6.51923
40	6.70603	6.59853
45	6.24357	6.23279
50	6.36456	6.34109
55	6.21245	6.1631
60	6.23155	6.18082

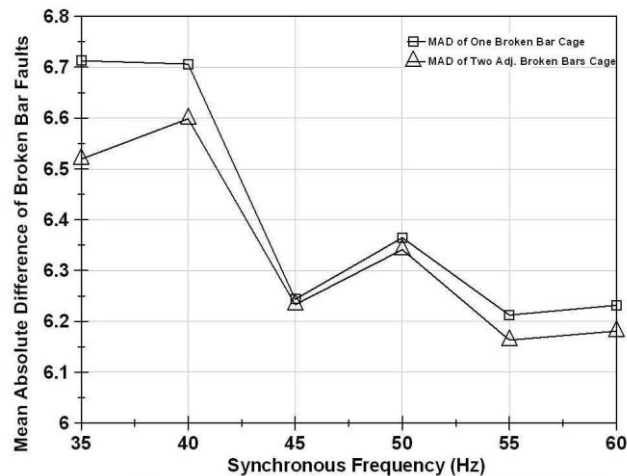


Fig.(16). MAD magnitude versus supply frequency.

5. Conclusion

In this paper, the Instantaneous Power Spectrum technique in the diagnosis of induction motor broken bar fault is investigated through sinusoidal and special inverter source. This investigation shows the performance of this technique in both cases. The method is effective on the diagnostics for the sinusoidal supply case, in contrast for the special inverter case. This result, leads to using one of the popular digital processing techniques, which is the Mean Absolute Difference Approach (MAD) to compare different spectrums against the healthy spectrum for hidden information's in the spectrum. The results were satisfactory, and show the potential of the proposed technique. The combined technique is very computationally efficient, and with the digital technology available now, an embedded system could be designed for that purpose with economical price.

6. References

- [1] Arfat Siddique, G. S. Yadava and Bhim Singh, "A Review of Stator Fault Monitoring Techniques of Induction Motors", *IEEE Trans. On Energy Conversion*, Vol. 20, No. 1, pp. 106 - 114, March 2005.
- [2] Subhasis Nandi, Hamid A. Toliyat and Xiaodong Li, "Condition Monitoring and Fault Diagnosis of Electrical Motors—A Review", *IEEE Trans. On Energy Conversion*, Vol. 20, No. 4, pp. 719-729, December 2005.
- [3] Vinod V. Thomas, Krishna Vasudevan and V. Jagadeesh Kumar, "Online Cage Rotor Fault Detection Using Air-Gap Torque Spectra", *IEEE Trans. On Energy Conversion*, Vol. 18, No. 2, pp. 265 - 270, June 2003.
- [4] A. Bellini, F. Filippetti, G. Franceschini, C. Tassoni and G.B. Kliman, "Quantitative Evaluation of Induction Motor Broken Bars By Means of Electrical Signature Analysis", *Industry Applications Conference, 2000. Conference Record of the 2000 IEEE*, Issue. 2000, Vol.1, pp. 484 – 491.
- [5] Mohamed El Hachemi Benbouzid, and Gerald B. Kliman, "What Stator Current Processing-Based Technique to Use for Induction Motor Rotor Faults Diagnosis?", *IEEE Trans. On Energy Conversion*, Vol. 18, No. 2, pp. 238 – 244, June 2003.
- [6] Hakan Çalış and Abdulkadir Çakır, "Rotor bar fault diagnosis in three phase induction motors by monitoring fluctuations of motor current zero crossing instants", *Electric Power Systems Research*, 77 (2007), pp. 385-392.
- [7] Zhenxing Liu, Xianggen Yin, Zhe Zhang, Deshu Chen and Wei Chen, "Online Rotor Mixed Fault Diagnosis Way Based on Spectrum Analysis of Instantaneous Power in Squirrel Cage Induction Motors", *IEEE Trans. On Energy Conversion*, Vol. 19, No. 3, pp. 485 – 490, September 2004.
- [8] Gaëtan Didier, Eric Ternisien, Olivier Caspary, and Hubert Razik, "Fault Detection of Broken Rotor Bars in Induction Motor Using a Global Fault Index", *IEEE Trans On Industry Applications*, Vol. 42, No. 1, pp. 79 - 88, January/February 2006.
- [9] J. F. Bangura and N.A. Demerdash, "Diagnosis and Characterization of Effects of Broken Bars and Connectors in Squirrel-Cage Induction Motors by a Time-Stepping Coupled Finite Element-State Space Modeling Approach", *IEEE Trans. On Energy Conversion*, Vol. 14, No. 4, pp. 1167 – 1176, December 1999.
- [10] Li Weili, Xie Ying, Shen Jiafeng, and Luo Yingli, "Finite-Element Analysis of Field Distribution and Characteristic Performance of Squirrel-Cage Induction Motor With Broken Bars", *IEEE Trans. On Magnetics*, Vol. 43, No. 4, pp.1537-1540, April 2007
- [11] Aderiano M. da Silva, Richard J. Povinelli, and Nabeel A. O. Demerdash, "Induction Machine Broken Bar and Stator Short-Circuit Fault Diagnostics Based on Three-Phase Stator Current Envelopes", *IEEE Trans. On Industrial Electronics*, Vol. 55, No. 3, pp. 1310 - 1318, March 2008.
- [12] Khmais Bacha, Humberto Henao, Moncef Gossa and Gérard-André Capolino, "Induction machine fault detection using stray flux EMF measurement and neural network-based decision", *Electric Power Systems Research*, 78 (2008), 1247/1255.
- [13] M.H. Song, E.S. Kang, C.H. Jeong, MY. Chow and B. Ayhan, "Mean Absolute Difference Approach for Induction Motor Broken Rotor Bar Fault Detection", *SDEMPED 2003, Symposium on Diagnostics for Electric Machines, Power Electronics and Drives*, Atlanta, CA, USA 24-26, pp. 115 – 118, August 2003.
- [14] Jeffrey Travis and Jim Kring, "LabVIEW for Everyone: Graphical Programming Made Easy and Fun, Third Edition", Prentice Hall.
- [15] Nasser Kehtarnavaz and Namjin Kim, "Digital Signal Processing System-Level Design Using LabVIEW", ISBN: 0-7506-7914-X.
- [16] NI™ *DIAdem Help*, April 2007 Edition.
- [17] Z. Ye, A. Sadeghian and B. Wu, "Mechanical fault diagnostics for induction motor with variable speed drives using Adaptive Neuro-fuzzy Inference System", *Electric Power Systems Research*, 76 (2006), 742/752.

تقنية مستحدثة لتشخيص كسر قضبان العضو الدوار للمحرك الحثي المستخدم في نظم خاصة للسرعة المتغيرة

حنفي حسن حنفي حسن^١، أحمد محمد حسين^٢، عصام الدين محمد أبو الذهب^٣، محمد أسامة خليل^٤

^{١،٣} قسم القوى والآلات الكهربائية - كلية الهندسة - جامعة القاهرة

^٢ قسم البحوث الكهربائية، معهد البحوث الميكانيكية والكهربائية، وزارة الري والأشغال العامة، مصر

^١Hanafy_Hassan@hotmail.com ^٢hussien_25@yahoo.com ^٣zahab0@yahoo.com ^٤m.khalil20@yahoo.com

(قدم للنشر في ٢٠٠٩/٣/١٢؛ وقبل للنشر في ٢٠٠٩/٦/٥ م)

ملخص البحث. يعرض هذا البحث تقنية مستحدثة لتشخيص كسر قضبان العضو الدوار ملخص البحث. للمحرك الحثي المستخدم في نظم خاصة للسرعة المتغيرة المزودة بملفات و مرشح جيبي عند أطراف الخروج والتي لا يمكن إلغائها وذلك لتقليل الاهتزازات المتولدة في المحرك. التقنية المقترحة تستخدم طريقة التحليل الطيفي للقدرة اللحظية بالتزامن مع آلية المتوسط الاختلافي المطلق. ولقد أوضحت النتائج العملية أن طريقة التحليل الطيفي للقدرة اللحظية فعالة فقط في حالة تغذية المحرك من مصدر له جهد جيبي ولم تكن فعالة في حالة تغذية المحرك من النظم الخاصة للسرعة المتغيرة الموضحة. يتم في التقنية المقترحة مقارنة التحليل الطيفي للقدرة اللحظية للمحرك السليم بالتحليل الطيفي للقدرة اللحظية للمحرك بعد كسر قضيب أو قضيبين من العضو الدوار للمحرك باستخدام آلية المتوسط الاختلافي المطلق لبيان مدى الاختلاف والتشابه بين الحالتين. ولقد أثبتت التقنية المقترحة فاعلية كبيرة في تشخيص كسر قضبان العضو الدوار للمحرك الحثي في حالة تغذية المحرك من النظم الخاصة للسرعة المتغيرة الموضحة.